DEUTSCHES ELEKTRONEN-SYNCHROTRON

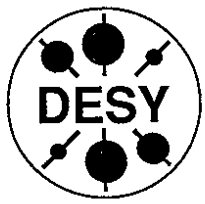

DESY 95-067
April 1995

The H1 Calorimetry: Performance and Upgrade Program

K. Borras
Institut für Physik, Universität Dortmund
M. Weber
Deutsches Elektronen-Synchrotron DESY, Hamburg

ISSN 0418-9833

NOTKESTRASSE 85 - 22607 HAMBURG

To be sure that your preprints are promptly included in the
HIGH ENERGY PHYSICS INDEX,
send them to (if possible by air mail):

DESY
Bibliothek
Notkestraße 85
22607 Hamburg
Germany

DESY-IfH
Bibliothek
Platanenallee 6
15738 Zeuthen
Germany

DESY 95–067
April 1995

ISSN 0418-9833

The Performance of the H1 Calorimeters

K. Borras
Institut für Physik, Universität Dortmund

The New H1 Spaghetti Calorimeter

M. Weber
Deutsches Elektronen-Synchrotron DESY, Hamburg

Invited talks given at the '94 Beijing Calorimetry Symposium'

The Performance of the H1 Calorimeters

K. Borras [a] , representing the H1 Collaboration

[a]Universität Dortmund,
D-44221 Dortmund, Germany

The energies of particles are measured in the H1 detector with four different calorimeters. Their designs, which are optimized for their particular requirements, are briefly described. Their performance is characterized in terms of their operational stability, the precision of their energy scale and their trigger functionality. The most important among the four calorimeters is the large liquid argon calorimeter and therefore most emphasis is given to the description of this component.

1. THE H1 CALORIMETERS

Since 1992 the HERA storage ring at DESY in Hamburg/Germany has made collisions between 27.6 GeV electrons (positrons) and 820 GeV protons with a time interval between bunch crossing of 96 ns. The physics program contains tests of the standard model up to regions of high momentum transfer ($Q^2 \approx 4 \cdot 10^4$ GeV^2) and low Bjorken-x ($\approx 10^{-4}$) as well as searches for new physics.

The H1 detector [1] is designed to achieve good measurements of the large variety of the physics processes. It provides among other features an excellent identification and measurement of electrons and muons. The energy of the produced particles is determined with four different calorimeters and these are optimally constructed according to their purpose and place in the detector.

Figure 1 shows a cross section of the H1 detector along the beam direction. The electrons (positrons), coming from the left side, and the protons from the right, collide in the interaction point indicated by a cross. The backward electromagnetic calorimeter (BEMC) detects mainly electrons scattered through small angles. The large liquid argon (LAr) calorimeter measures electrons scattered through larger angles and most of the hadronic energy flow. Very forward hadrons are detected in the plug calorimeter. These calorimeters are surrounded by the iron yoke, which is instrumented with limited streamer tubes, that serves as a muon detector and as a calorimeter (tail catcher) for hadronic energy leaking out of the inner calorimeters.

2. THE LAR CALORIMETER

One of the main components of the H1 detector is the large LAr calorimeter. It is described in detail in [2].

2.1. Construction and subsystems

The LAr calorimeter consists of an electromagnetic (EMC) and a hadronic (HAC) section (fig. 1). The electromagnetic section is built as a pile of absorber boards with a lead kernel of 2.4 mm and liquid argon gaps of 2.35 mm. Its depth varies between 20 and 30 X_0 (1.3 λ). The hadronic section consists of 19 mm thick stainless steel absorber material, the calorimeter signal being read out in a double liquid argon gap of 2×2.4 mm thickness. The total depth for hadrons including both sections amounts to 4.5 – 8 λ. In order to account for the average flight direction of the produced particles, the plates, and therefore the gaps, are oriented perpendicular to the beam direction in the forward and backward part and parallel in the central barrel region. The whole absorber structure and LAr volume of 53 m^3 has a weight of about 600 tons.

The LAr calorimeter is divided into eight self supporting wheels (fig. 1), each of them consisting either of two half rings or of eight individual octants. The fine segmentation of the H1 LAr calorimeter leads to 44 352 read out channels.

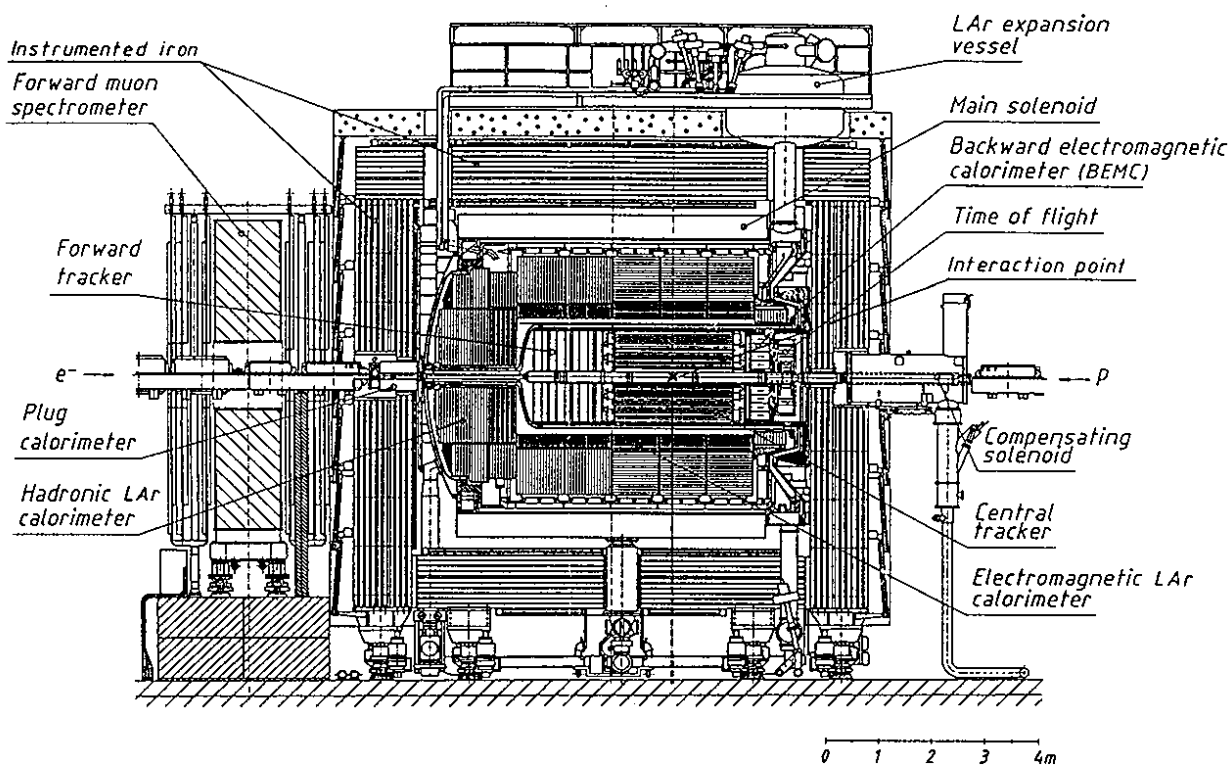

Figure 1. Cross section of the H1 detector along the beam direction.

The LAr calorimeter is operated with several monitoring and data acquisition (DAQ) computer subsystems. The HV–supply, LAr–purity and the slow control are monitored by three different systems, which are controlled by one OS9 system. The slow control monitors and controls all electronic components. When there is a fault the slow control provides information about the location of the problem, hints for repair and names of experts to be called. The performance of the other two monitoring subsystems are described in the following sections.

The DAQ subsystems are the front end electronics, the energy signal read out and the calorimeter trigger branch. All three are controlled by the calorimeter OS9 system, which is steered during luminosity running by the central H1 DAQ, but can also be used in stand alone mode or together with a VAX station for tests.

2.2. The HV–system

The whole calorimeter is supplied by 1504 individual high voltage lines. They are served by 56 sources each feeding a distributor with 32 output channels. On average each octant of an electromagnetic or hadronic wheel uses 12 lines. The calorimeter cells are connected from 2 to 12 lines. Therefore no part of the calorimeter is completely inactive when there is a problem with one high voltage line. The currents drawn are monitored by an OS9 system via a VME–bus interface. The threshold for an overcurrent is 2 μA for an operating voltage of 1500 V. If an overcurrent is detected, the line is connected to one of the special distributors, which can supply 200 μA in sum for all channels instead of 20 μA from the usual distributors. The special distributors are driven

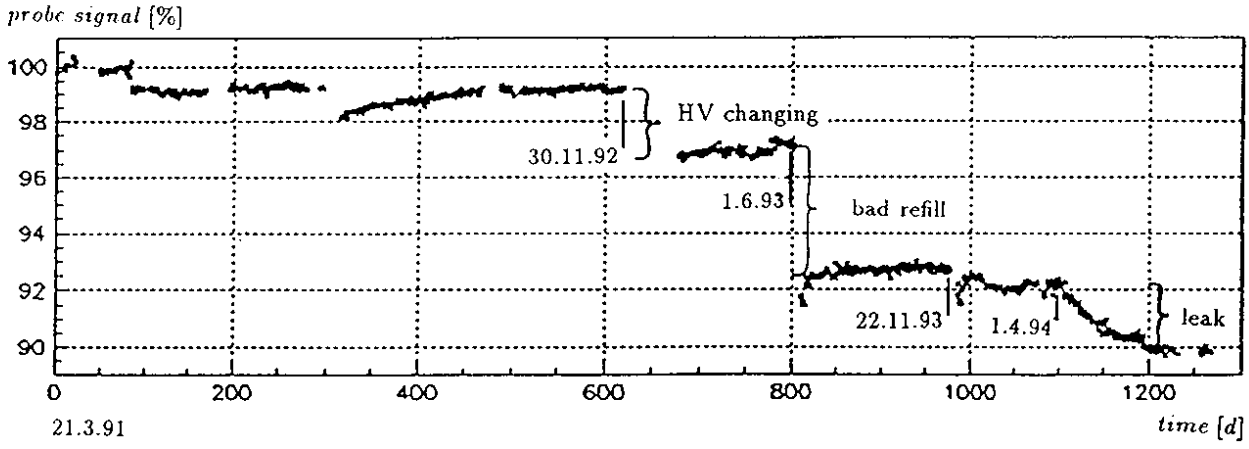

Figure 2. Development of the purity since January 1991 (suppressed zero).

by the nominal (1500 V) or the reduced (1000 V) voltage for lines drawing higher currents up to 100 μA per line. Presently 59 (4%) lines are running at 1000 V and only 3 (0.2%) have had to be disconnected. This status has been stable from July 1994 until the end of the luminosity period (1.November 1994).

2.3. The LAr–purity monitoring

The LAr calorimeter started operation in January 1991. It has been kept cold and full of LAr except for shut down periods, where the moving of the detector out of and into the beam region required emptying of the cryostat. The same LAr load has been kept since the beginning without purification. There are 11 small ionisation chambers positioned in the cryostat. They are used to monitor the LAr–purity by measuring the energy spectra of the radioactive decays of α or β sources. The amplitude is measured continuously with a constant HV setting. As can be seen in figure 2 the largest losses of signal height are caused by failures during the extracting and refill operations. During the luminosity conditions in 1994 the status was stable with a small ageing effect of about 0.8% per year. Over the 3.5 years of operation only about 10% of the signal height has been lost in total due to the increase of the impurity.

This result is also confirmed by a second operation mode of the probes. Here, about 5 times per year, the amplitude is measured as a function of the HV applied to the probes. The analysis of the HV/amplitude dependence yields the charge collection at an infinite electrical field and also the impurity. At present the impurity amounts to about 1 ppm. The same method can be used with the calorimeter itself. By analyzing the response of cosmics as a function of the HV applied to the calorimeter gaps in the test running phase 1991/1992 a charge collection efficiency of about .944±0.014 at the nominal voltage of 1500 V, corresponding to an electric field of 625 V/mm in the LAr gap, was determined. Converting the results of the purity probes to the calorimeter gaps, the charge collection efficiency is presently about .879±0.015 at the nominal voltage.

2.4. The data readout

The 44352 calorimeter cells are read out via ganging cables connected to the gaps of the cells and a merging board, where the regrouping of the final configuration is done. Approximately 3000 signal cables are fed through special feedthroughs to boxes located directly at the cryostat. In these analog boxes the signals are first amplified and then split into the normal data path, briefly outlined in the following, and the trigger path, described in the next section.

In the data path the signals are shaped, twofold multiplexed and sent via two differentially driven twisted pair cables of about 25 m to the analog receiver units in the electronic trailor. Then the signals are digitized by ADC's and processed by fast Digital Signal Processors (DSP). The latter perform pedestal subtraction, powerful data reduction by noise suppression and electronic calibration corrections. Only about 90 (0.2%) channels can not be read out and about 20 channels are noisy. All channels are continuously monitored by the analysis of events taken with random triggers and corrected during the offline data reconstruction.

The noise introduced by the electronic chain depends on the cell sizes, the following table 1 gives the averaged values.

Table 1
Average electronic noise per calorimeter cell.

calorimeter	region	
type	central barrel	forward
EMC	34 MeV	10 MeV
	(0.33 mip)	(0.10 mip)
HAC	28 MeV	18 MeV
	(0.15 mip)	(0.11 mip)

The calibration of the electronic chain is performed by measuring the ADC response to known charges injected via capacitors at the merging boards or at the preamplifier level. The charge generators work at a high precision level of (0.1–0.2)%. For each channel a third order polynomial fit with four parameters describes the dependence of the measured ADC signal from the injected charge. The parameters are loaded into the DSP's, where the ADC signals are converted into charge equivalents. The calibration system is also used to determine the electronic corrections needed for cross–talk.

The calibration is checked at least every second day. During 1994 the calibration was updated about 20 times. Most updates were necessary because of hardware replacements. Otherwise the calibration is stable. Usually a new calibration is performed for the full calorimeter once per month.

The data acquisition system achieves a maximum rate of 250 Hz. A rate of 5 Hz is achieved when reading out special data for noise analysis. This is slow because every calorimeter cell is read out without noise suppression making a total event size of up to 200 kbytes. During luminosity operation the effective noise suppression delivers only about 9 kbytes per event, which are read out with the average rate of 30 Hz of the central H1 DAQ.

2.5. The LAr trigger

All calorimeter cells are grouped into 5009 trigger cells. 656 trigger towers (TT) are built by the summed and shaped signals of up to 4 electromagnetic and 6 hadronic trigger cells. The TT's are further grouped into 256 big towers (BT). Information from the TT's is only gated by fast analog switches and passed to the BT's, if the threshold (currently set to 1.2 GeV) is exceeded. The signals of the BT's are digitized in FADC's. Figure 3 shows the good correlation between the energy measurement in the trigger FADC's and in the data path. No systematic deviations are visible.

Since the LAr calorimeter is a non–compensating calorimeter the energies in the EMC and HAC BT sections are added after relative weighting with look–up tables. They are used to calculate trigger elements such as the energies in the different parts of the calorimeter, transverse energy, missing transverse energy or an electron trigger. These trigger elements are discriminated at three levels of thresholds. The trigger decision takes about 21.5 bunch crossings (about 2.1 μs). The performance of the time determination with the calorimeter trigger is demonstrated in figure 4, where the timing over the full angular range of the calorimeter is shown. The given quantity t_0 is the nominal bunch crossing added by 5. For an optimal timing t_0 should have a value between 4 and 5. The resolution is on average 20 ns.

2.6. Checks for the energy calibration

The energy calibrations for all wheel types were derived from test beam measurements at CERN,

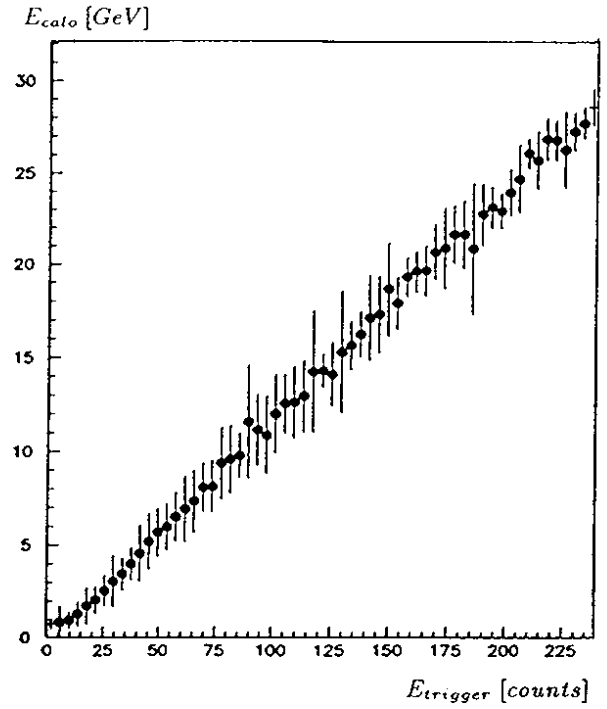

Figure 3. Correlation between the energies measured in the data path and in the trigger.

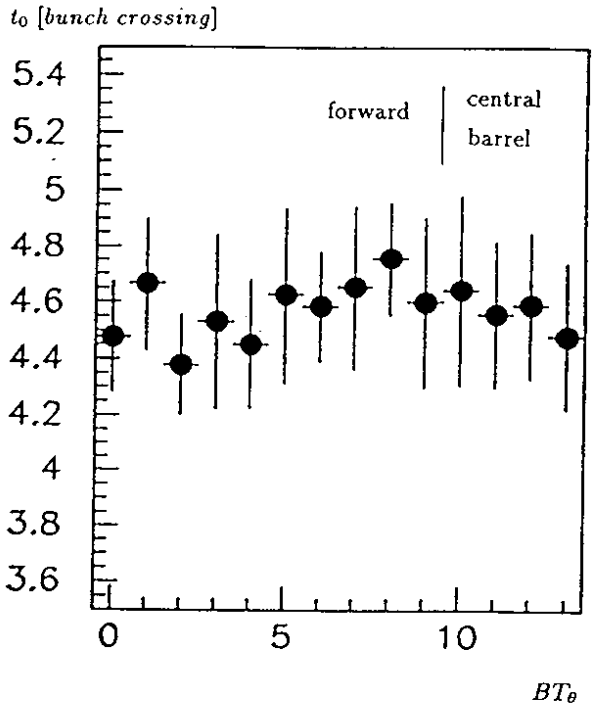

Figure 4. Calorimeter trigger timing as a function of the BT–index θ.

as described in [3]. More details can be found in [4,5]. The determined calibration constants were transfered to H1 without changes and are still valid. In this section some checks for the precision of the energy scale are given.

Among the events produced by HERA ep–collisions there are no special calibration processes like Bhabha–scattering available. Also precision tests with resonances similar to the Z^0–peak analyses were not possible. But there are several other checks to determine the precision of the energy scale.

Cosmic muons, traversing the H1 detector, can radiate low energetic electrons. Their momentum, as measured in the tracker, can be compared to the energy, reconstructed in the calorimeter. Figure 5 shows results of an analysis of such events. In the first picture the data are compared to simulations which are assumed to give the ideal energy scale [4,5]. The good agreement for data and simulation with a ratio of the mean $E_{calorimeter}/P_{tracker}$–values of 0.99±0.012 confirms the energy scale for low energetic electrons. In the lower picture the results for data taken in 1993 and 1994 are compared. Inspite of the additional impurity caused by a leak (fig. 2) the mean values of the reconstructed ratios are identical on the 1%–level. This confirms the correction method applied for the higher impurity in 1994 in the offline data reconstruction.

For high energetic electrons in ep–collisions, one can employ the double angle method: in neutral current events the energy of the scattered electron can be determined by its scattering angle against the incoming proton direction and the scattering angle of the outgoing current–jet. This evaluated electron energy was compared to the energy measured in the calorimeter and the agree-

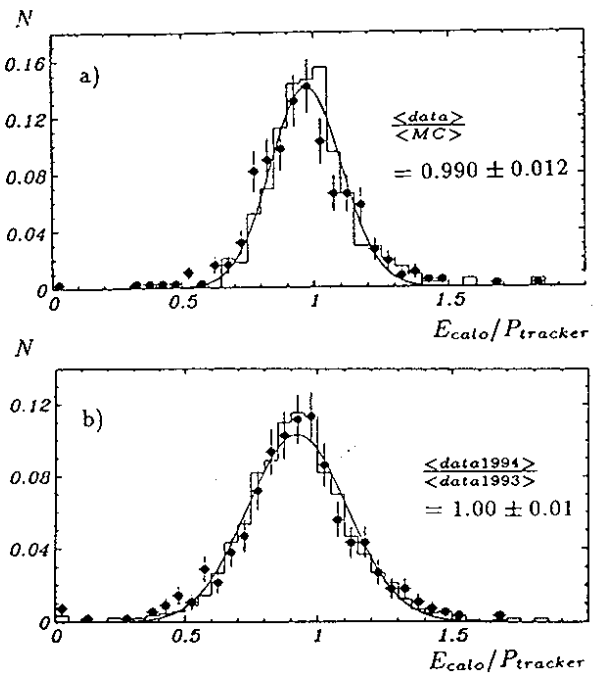

Figure 5. Ratio of $E_{calorimeter}$ and $P_{tracker}$ for electrons radiated by cosmics, comparison a) 1994 data(points) and simulation(histogram) and b) 1993 (histogram) and 1994(points) data.

ment is better than 1%.

One check for the precision of the hadronic scale was performed by comparing the transverse momentum of the scattered electron with the vectorial sum of the transverse momentum of the hadronic final state. Both should be balanced in neutral current deep inelastic scattering events. For figure 6 two cases were distinguished: the low energetic case with a p_{el}^T between 10 and 20 GeV and the high energetic case with p_{el}^T larger than 20 GeV. As mentioned in [3] almost all CERN test and calibration data were taken in the high energy range, where the agreement between data and simulation is very good.

In summary, including other tests based on smaller statistics, the electromagnetic energy scale precision is better than 3% and the hadronic energy scale precision is better than 6%.

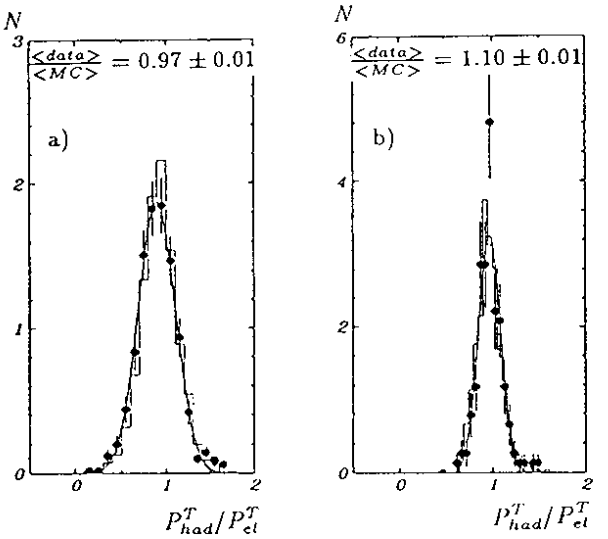

Figure 6. p^T-balance for neutral current events with a) 10 GeV < P_{el}^T < 20 GeV and b) P_{el}^T > 20 GeV for data(points) and simulation(histogram).

3. THE TAIL CATCHER

The return yoke of the main solenoid magnet surrounds the central H1 detector components (fig. 1) and is instrumented with layers of limited streamer tubes (LST). Their purpose is twofold: first the detection and survey of tracks of penetrating muons and second the measurement of hadronic energy leaking out of the inner calorimeters. According to their different purposes the streamer tube read out is built either by strips perpendicular to the wires for track reconstruction or by pads of the size $40\times50\text{cm}^2$ or $25\times25\text{cm}^2$ for energy measurement. The nine slits of the iron yoke are filled with layers of LST with pads. In addition in front and behind the iron one layer of pad read out is complemented with 2 layers of LST's with strips. Also in the middle of the iron structure one layer with strips is added to the pad layer. The first five and the last six pad layers are grouped together such that a geometry of projective towers is achieved. The analog signals of the 3888 channels are, after amplifica-

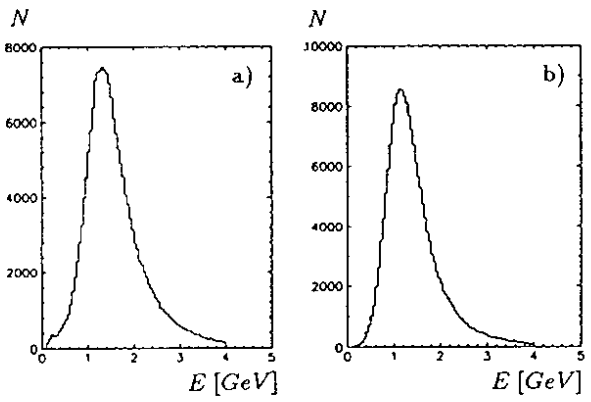

Figure 7. Muon spectra(histogram) for a tower with 6 (a)) and 5 (b)) layers.

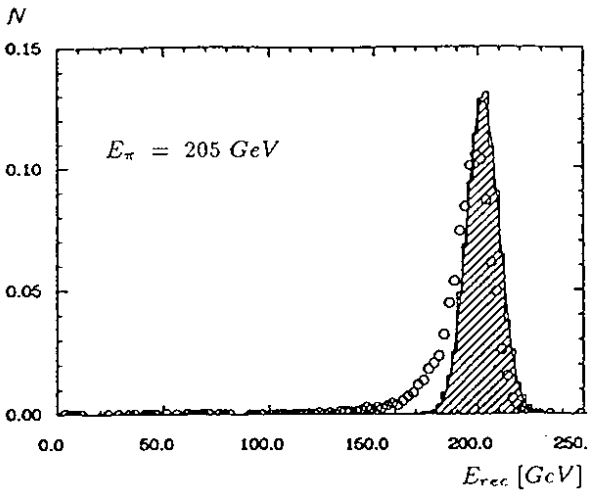

Figure 8. Energy reconstructed with(hatched histogram) and without(circles) the tail catcher for 205 GeV pions in the test beam measurements.

tion, shaping and multiplexing, read out through the same chain than the LAr signals. The wires and strips are read out and treated in a separate data and trigger path. With the 10 iron layers of 7.5 cm thickness the active depth of the tail catcher amounts to about 4.5 λ.

The LST are operated with a non–flammable gas mixture of 85% CO_2, 9.5% Isobutane and 2.5% Ar. This mixture, instead of the standard 75% Isobutane and 25% Ar mixture, provides acceptable performance for the charge spectra and efficiencies for muons as well as for the measurements of the hadronic shower tails. The performance in detecting and measuring muons is demonstrated in figure 7, where it is obvious that the signals for muons are well separated from noise: the clean muon signal is Landau like distributed with means and most probable values far beyond the pedestals. The width relative to the most probable value is about 39%. The ratio of the mean values for the two different tower sizes corresponds to the expected value of 0.83.

The usage of the non–standard gas mixture is the reason for a significantly reduced HV plateau width. Therefore the calorimeter response is very sensitive to temperature and air pressure. These and also the quality of the gas mixture are very carefully monitored and the HV is adjusted accordingly. In analyzing the signals from halo muons continuously during the luminosity period 1994 a stability of better than 2% was found which proves the good functioning of this operation.

To achieve uniformity of the tail catcher response intercalibration constants for each tower were determined by using cosmics. These intercalibration constants varied from 1993 to 1994 to within 3%. The energy calibration was taken from test beam results measured at CERN. Figure 8 [4] shows one result concerning the measurement of hadronic energy leaking out of the LAr calorimeter. For pions with an energy of 205 GeV the inclusion of the tail catcher response improves the mean value and reduces the tail of the reconstructed energy considerably. The energy scale of the tail catcher was checked in a similar way than the hadronic scale of the LAr hadronic energy scale. Here also the p^T–balance was used and figure 9 shows the ratio of p^T_{had}/p^T_{el} for the data taken in 1994 as a function of the energy fraction reconstructed in the tail catcher. No significant dependence on this fraction is visible. This confirms the energy scale on the 5%–level.

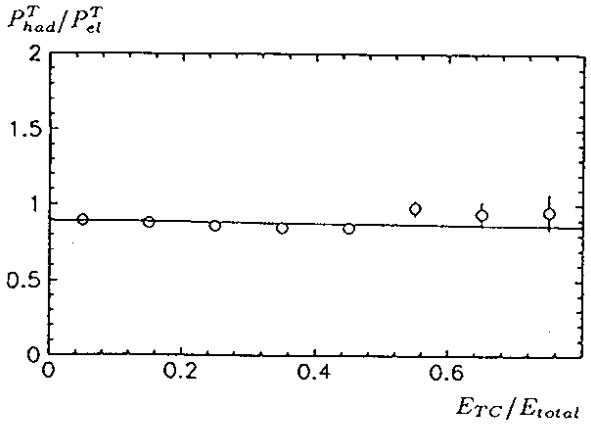

Figure 9. p^T–balance as as function of the energy fraction in the tail catcher (TC).

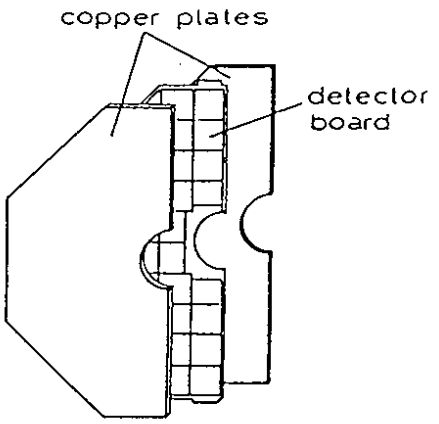

Figure 10. Exploded view of a detector module.

4. THE PLUG CALORIMETER

In order to get an energy measurement in the forward direction of the H1 detector between the beam pipe and the LAr calorimeter a small and compact copper–silicon calorimeter is used. Its inner radius is 6 cm and its outer one is 32 cm. The length of 69 cm corresponds to 4.25λ and 44.6 X_0. Because of the cryostat walls and the beam pipe there is a large amount of inactive material in front of the plug calorimeter. Therefore the first active silicon plane starts in front of the detector and not in the first slot. In 1994 the plug calorimeter was fully instrumented for the first time. In 8 planes divided into half discs (fig. 10) 648 silicon–detectors were installed and their signals collected into 330 channels read out as a branch of the electronic analog chain of the H1 calorimeters with the same components.

The energy calibration is based on the determination of the visible energy with α–particles and for the absolute energy deposition on detailed simulations compared to test measurements. For the data taken in 1993 figure 11 shows a good agreement for the energy deposition in the plug calorimeter between deep inelastic scattering data and simulations. The plug calorimeter is also used as a veto for diffractive events, which are characterized by no energy deposition in the forward region of the detector. For this purpose a low noise level is required. Therefore noisy channels are monitored and removed in the reconstruction. Without this noisy channel treatment the distribution of the reconstructed energy has a mean value of –0.14 GeV and shows a quite large sigma of about 4.8 GeV. Taking out the monitored noisy channels the energy distribution has a mean value of –0.02 GeV and a sigma reduced by nearly an order of magnitude to 0.65 GeV.

More noisy channels than expected were found during the luminosity period 1994. Therefore a detailed analysis of the silicon–detectors by measuring the capacity/voltage–characteristic in situ was started even before the end of the 1994 data taking period. As a result it was found that 59 (9%) detectors were damaged. The first layer nearest to the interaction point being more affected than the last layer and also the detectors close to the beampipe showing a higher amount of damage than the outer ones. A possible reason could be a combination of variations in the silicon–oxidation quality and radiation damage due to the higher luminosity in the data taking period 1994. After the luminosity running all the silicon–detectors were removed for further tests.

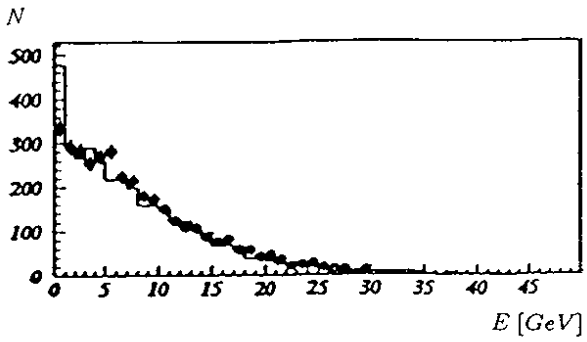

Figure 11. Comparison of the energy deposition in the plug calorimeter for 1993 data(points) and simulations(histogram).

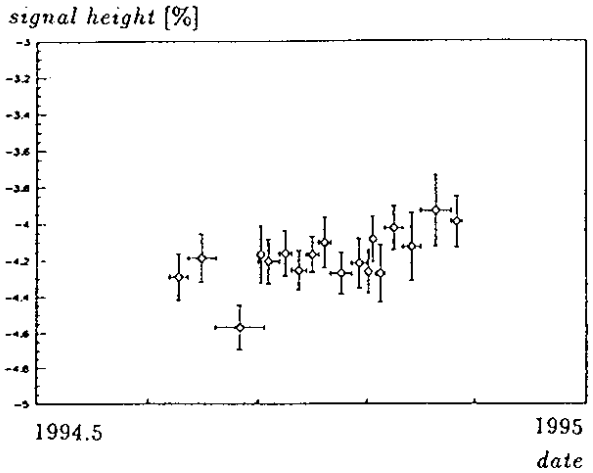

Figure 12. Signal height with time in the BEMC.

5. THE BEMC CALORIMETER

A conventional lead–scintillator–sandwich calorimeter covers the region between the LAr calorimeter and the beampipe in the backward direction (fig. 1). It is optimized to measure precisely the energy of scattered electrons in deep inelastic collisions with low Q^2, which implies a small scattering angle for the electron. Together with the tail catcher the BEMC contributes also to the measurement of hadronic final states.

The 50 active sampling layers of 4 mm thick SCSN–scintillator, interleaved by 2.5 mm thick lead sheets, are put into stacks oriented parallel to the beam pipe. 56 of the 88 stacks have a quadratic shape of $15.9 \times 15.9\ \mathrm{cm}^2$, the rest with a trapezoidal or triangular shape complete the overall shape to a circle with a diameter of 162 cm. The scintillator light is read out with 4 wavelength shifters (WLS), where 2 WLS are mounted on opposite sides in quadratic stacks and cover the whole length of 22 X_0 (0.97λ). A separate measurement of the shower tail is provided by the other 2 shorter WLS, which collects light from the last 6.8 X_0. The WLS are read out by photodiodes coupled to charge sensitive preamplifiers. The signals are received in the electronic trailor by a special analog card, which forms an unipolar signal faster than that of the LAr calorimeter, in order to generate a fast trigger signal. The remaining components of the read out chain are similar to the LAr system. The timing of this read out is very important for the absolute energy scale, since a shift of 30 ns would cause a shift of 1% in the energy scale. The total of 472 channels are aligned to 2.4 μs within 10 ns and the check of this timing revealed only a very small mean shift of less than 1 ns.

The electronic calibration is done with a pulsing system identical to that of the LAr calorimeter. In total 8 calibrations were performed during the luminosity period 1994, but without them the drifts would have been smaller than 0.5 permill. The energy calibration can be precisely adjusted by using deep inelastic scattering events. Due to kinematics a high amount of scattered electrons have an energy around the electron beam energy (kinematic peak), which is seen in the energy distribution of the scattered electrons. Using simulations the absolute energy scale of the BEMC could be adjusted to a precision of 1%. In 1994 enough statistics was accumulated to determine the stability of the signal height with time. The signal was stable on the 1%–level during the 1994 luminosity operation with positrons (fig. 12).

A special trigger had to be developed for this calorimeter, since it is exposed to a high background rate from beam–wall and beam–gas in-

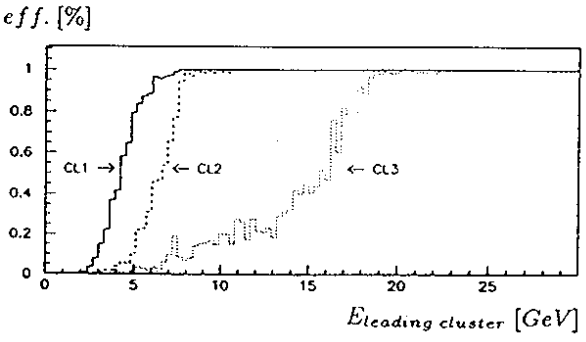

Figure 13. Efficiencies for the BEMC trigger.

teractions. The rate of deep inelastic scattering events is in contrast about 5 orders of magnitude smaller. The BEMC trigger looks for well localized energy depositions in neighbouring stacks (clusters) at three different thresholds. The thresholds for the 50%–efficiencies of the three levels of cluster energy triggers are: CL1 : 4.3±1.1 GeV, CL2 : 7.7±1.0 GeV and CL3 : 16.9±1.6 GeV. Among them the CL2 trigger is the most used one and it reaches its full efficiency (50%+2σ) at 9.7 GeV (fig. 13). The timing of the trigger is well adjusted within 3 ns.

6. SUMMARY

As demonstrated all H1 calorimeters show a satisfactory performance.

The LAr calorimeter has been in operation since January 1991. There has been about 10% loss of signal on the purity probe level over the past 3.5 years. The drop is mostly due to failures during the movings of the detector. During the luminosity operation 1994 a signal loss of about 0.8% per year is achieved. On the calorimeter level the charge collection efficiency decreased from .944±0.014 to .879±0.015 at the nominal voltage of 1500 V, corresponding to an electric field of 625 V/mm, during the operation time. Although there are no classical calibration processes available and the performed checks are limited by statistic, the precision of the energy scale could be determined to be better than 3% for the electromagnetic and better than 6% for the hadronic scale.

The response of the tail catcher was in 1994 stable to within 2%. Its absolute energy scale was checked with the p^T–balance method on the 5%–level.

The plug calorimeter was fully instrumented for the first time in 1994 and could be operated well. The number of silicon–detectors damaged during the luminosity operation is higher than expected and presently under study, but is via monitoring and software correction under control.

Also the backward calorimeter BEMC showed a stable energy response to within 1% during the luminosity operation with positrons. Using the kinematic peak the electromagnetic scale could be adjusted with a precision better than 1%.

These performance results show that the design goals for the H1 calorimeters are close to being achieved.

Acknowledgements

I am grateful to my colleagues of the H1 Collaboration who let me show results based on their combined effort to build, test and operate such a large detector. This work was supported by the Bundesministerium für Forschung und Technologie, Germany (grant-no: 6DO57I).

REFERENCES

1. H1 collab., The H1 detector, DESY 93-103.
2. H1 calo. group, NIM A336 (1993) 460-498.
3. W.Braunschweig, The H1 liquid Ar detector and Cryogenic calorimetry for LHC experiment, proceedings of '94 Beijing Calorimetry Symposium'.
4. H1 calo. group, NIM A336 (1993) 499-509.
5. H1 calo. group, NIM A344 (1994) 492-506, NIM A350 (1994) 57-72.

The new H1 Spaghetti Calorimeter

Marc Weber,[a] representing the H1 collaboration

[a]DESY, Notkestraße 85, D-22603 Hamburg, Germany.

The H1 collaboration is building a new calorimeter which will be installed in the backward scattering region of the H1 detector in the winter shut-down 1994/95. The calorimeter consists of 0.5 mm diameter scintillating fibers embedded into lead plates. The lead to fiber ratio is 2:1. The main design goals for the calorimeter are an energy resolution of better than 2% for 30 GeV electrons and a geometric acceptance up to electron scattering angles of 2.5° with respect to the beam pipe. The design and the construction of the calorimeter is reviewed and the performance of final detector modules in test measurements is presented.

1. INTRODUCTION

The new accelerator ring HERA at DESY collides 27 GeV electrons or positrons with 820 GeV protons. HERA is the ideal tool to study electron-proton reactions at high values for the four-momentum transfer variable Q^2 which have not been accessible to fixed target experiments. Due to the large proton momentum the event particles are boosted in the proton direction – the forward direction. Consequently the instrumentation of the H1 detector is asymmetric as can be seen from Figure 1, where a standard deep inelastic scattering event is shown. The electron beam enters the detector from the left, the protons from the right side. The scattered electron is visible as an isolated track in the central tracking detectors and as an energetic cluster in the backward electromagnetic calorimeter (BEMC). The struck parton has fragmented into a jet of particles directed into the forward region.

With the growing interest in low x physics [1] an improved measurement of events where the electron strucks a soft parton inside the proton and the generated particles might be boosted in the backward (electron) direction was requested [2].

The H1 collaboration has therefore started an ambitious upgrade programm of the backward part of detector. In particular the existing lead-scintillator-sandwich calorimeter, the BEMC, will be replaced during winter-shutdown 1994/95. The required performance of the new calorimeter and its construction techniques will be described below.

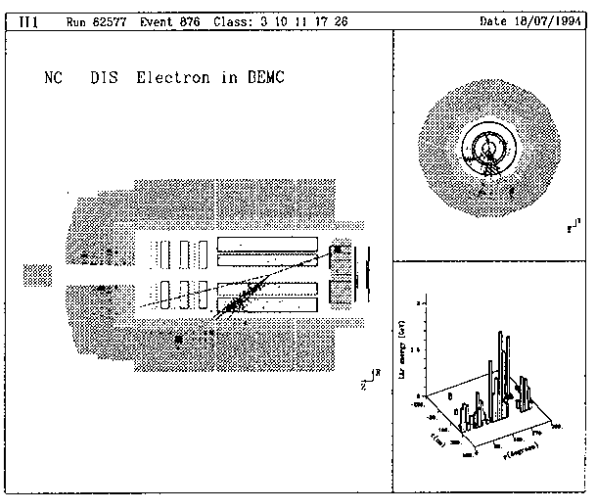

Figure 1. A deep inelastic scattering event recorded with the H1 detector with the scattered electron observed in the backward calorimeter (on the right side of the detector).

2. PHYSICS MOTIVATION

The main features of the new calorimeter in comparison to the BEMC are the following:

- A large geometric acceptance covering electron scattering angles larger than 2.5° which will extend the measurements of the proton structure function F_2 down to very low x values.
- A much improved electromagnetic energy resolution of better than 2 % for electron energies of 30 GeV in combination with an absolute energy calibration of 0.5% and a spatial homogeneity close to 2 % is essential to keep the systematic uncertainties of the F_2 measurements in the range of 5 - 10% [3].
- A position resolution in the millimeter range which corresponds to an angular resolution of the scattered electron of a few mrad.
- A reliable electron–pion separation is needed to suppress background events from photoproduction which are several orders of magnitudes more abundant than deep inelastic scattering events. Pions from photoproduction may thus be a source of fake electrons in the backward region.
- A time resolution of less than 1 ns independent of the particle energy i. e. for high energetic electrons, interacting pions as well as for minimum ionizing particles to suppress upstream proton background already at the first trigger level.
- The measurement of hadrons which allows us to determine the kinematic variable y without using the electron information. This offers the possibility to make cross checks and to identify radiative events with an additional photon radiated by the initial or final state electron.

A summary of the design characteristics is given in Table 1.

Table 1
Design goals

Acceptance	$153° < \theta < 177.5°$
σ /E	$7\%/\sqrt{E} \oplus 1\%$
e/π separation	$\epsilon_e/(1-\epsilon_\pi) > 100$
Time resolution	< 1 ns
Position resolution	a few mm
Angular resolution	2 mrad
Absolute calibration	0.5 %

3. DESIGN AND CONSTRUCTION

Two different calorimeter types were seriously considered to be good candidates to fulfil the requirements discussed above — a lead fluoride cristal calorimeter and a spaghetti calorimeter (Spacal). Prototypes for both options were built and investigated in detail [4,5]. The main reason to favour a spaghetti type calorimeter were the high cost and the restricted hadronic response of the cristals.

The exact position of the Spacal within the H1 detector is shown in Figure 2.

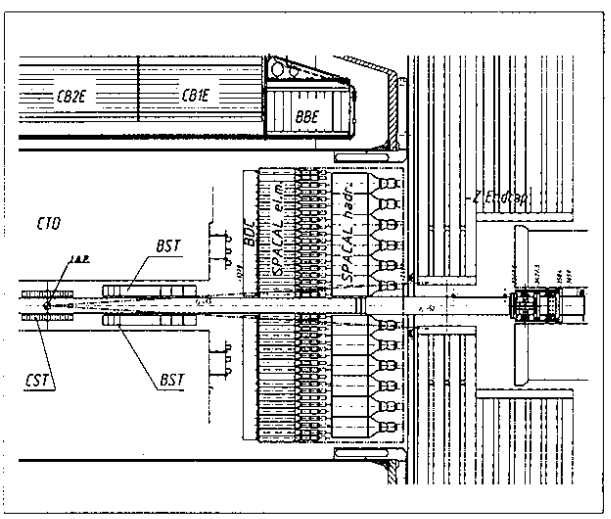

Figure 2. Extended view of the backward region of the H1 detector showing the two Spacal sections.

The two different sections of the Spacal – electromagnetic and hadronic ones – provide the lon-

gitudinal segmentation useful for particle identification. The fiber bundels, light mixers and photomultipliers of the electromagnetic section are directly in front of the hadronic one and have to be kept as compact as possible. This report will concentrate on the description of the electromagnetic section, which performs the main task of the Spacal, the precise measurement of the scattered electron.

3.1. Submodule production

The basic unit of the electromagnetic calorimeter is a block of 52 lead plates (see Figure 3), called a submodule. Each lead plate has 90 grooves with scintillating fibers put into it. The fibers are grouped into two bundles with a length of 80 mm held in a bundling frame. The bundle ends are coupled by an air gap of 0.3 mm to the light mixers glued to photomultipliers (not shown in the figure). The standard cell size of the electromagnetic section is $40.5 \times 40.5 \times 250$ mm^3.

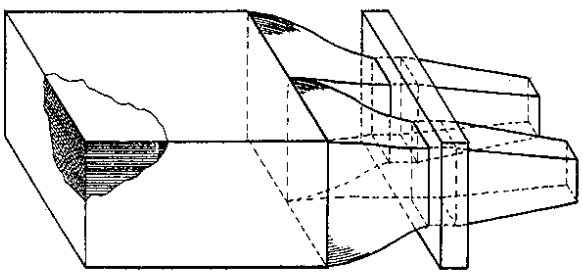

Figure 3. Schematic view of a submodule, the smallest detector unit.

The diameter of the scintillating fibers is 0.5 mm, the lead to fiber volume ratio of the detector is 2:1. Due to the small fiber diameter a high sampling frequency is obtained which allows us to obtain the required energy resolution with a sampling term close to $7\%/\sqrt{E(\mathrm{GeV})}$. The choice of the lead to fiber ratio is a compromise between aiming for an even smaller sampling term or for a more compact calorimeter. Having chosen the fiber diameter and the lead to fiber ratio, the radiation length and the Molière radius of the Spacal are 0.91 and 2.55 cm, respectively. A summary of the main construction parameters is given in Table 2.

In Figure 4 the profile of the lead plates and the fiber position in the plates is shown. The lead plates are produced with a special rolling machine at DESY constructed using the experience of [6]. The quality of the mechanical tolerances of the plates is essential for the performance of the detector. The height of our lead plates is constant to a precision of a few microns. This is at the limit of what is technically realizable today.

Various fibers from different producers were studied with detailed β–source scans [9,10]. The most important fiber properties were a long attenuation length to avoid a signal dependence on the position of the shower maximum, small light yield fluctuations from fiber to fiber which compromise the constant term of the energy resolution and sufficient radiation hardness. Our final choice was the fiber type BCF-12 from BICRON.

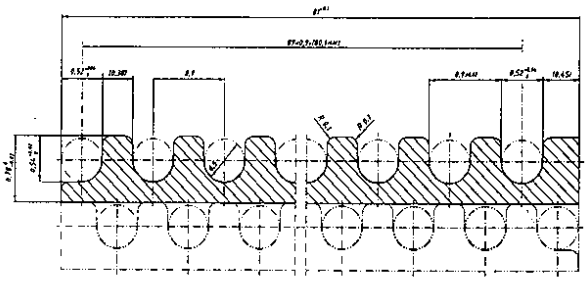

Figure 4. Front view of a lead plate with the grooves for 0.5 diameter scintillating fibers.

A compilation of the results for two different fiber types is shown in Figure 5. For these measurements the fiber length was 30 cm. A considerable increase of the light yield and the attenuation length is observed for fibers mirrored at the end opposite to the photomultiplier. The measured attenuation length is close to three meter for BCF-12 fibers which is largely sufficient for our detector. For all measurements the scintillation light reflected by the cladding of the fiber, which has an attenuation length considerably shorter than the core light, was absorbed by

Table 2
Construction parameters

	Electromagnetic section	Hadronic section
Fiber diameter	0.5 mm	1.0 mm
Lead/fiber ratio	2 : 1	4 : 1
Number of channels	1192	128
Size of standard cell	40.5×40.5 mm^2	120×120 mm^2
Radiation length	0.91 cm	-
Interaction length	25 cm	20 cm
Active length	25 cm	25 cm
Molière radius	2.55 cm	-

a strip of black paint at the fiber end near the photomultiplier.

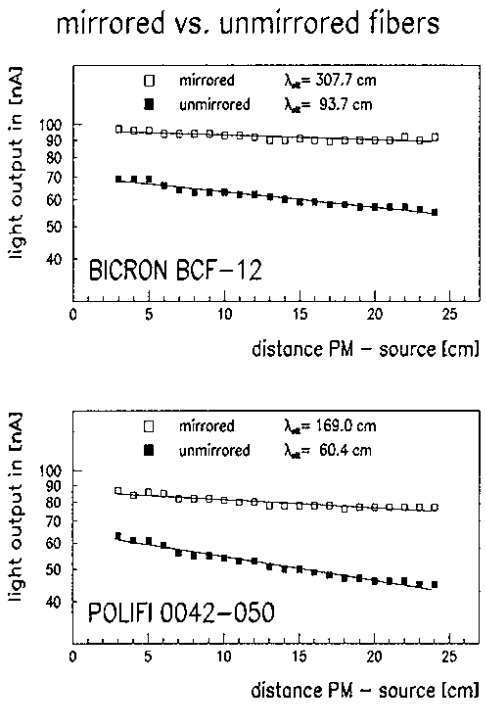

Figure 5. Light yield and attenuation length measurements for two different fiber types, both with and without mirrored fiber ends.

In the following, the main steps of the submodule production are summarized: The mirrored fibers are put into the grooves of the lead plates. The fibers are fixed in the grooves by a thin strip of acrylic glue near the front side of the lead plate. At the PMT side an approximately 1 cm wide strip of black epoxy glue absorbs the cladding light of the fibers and gives mechanical stability. After the preparation of 52 plates, the plates are put into a stacking form, which is then pressed horizontally and vertically with a weight of 1.5 tons. This procedure avoids the uncontrolled deformation of the final detector after its assembly. The stacked lead plates are then stabilized by a layer of 60 μ thick tape surrounding the module. Last, the fiber ends are bundled and glued together with blackened epoxy glue.

3.2. Supermodule production

Eight submodules are combined to form a 16–channel supermodule. By selecting submodules with matching geometrical tolerances, the module cross section of 162.6×162.6 mm^2 is kept within a typical tolerance of 0.1 mm. Next, the back side of the supermodule with the fiber bundles is machined to form a flat optical surface. The supermodule is wrapped in two more layers of tape similar to the submodules. The supermodule production is completed by adding a housing which contains 16 light mixers and PMTs to the machined fiber bundles. A high voltage distribution board and a light calibration module are mounted at the back of the PMT housing.

In Figure 6 a block of four supermodules together with a PMT housing and one of the PMTs on the top of the detectors is shown. The submodule structure of the detector is clearly visible from the front side.

3.3. Channeling

An intrinsic property of all scintillating fiber calorimeters is the channeling effect – the signal dependence on the angle between the impinging particle direction with reference to the fiber orientation. The most extreme scenario is a particle traveling along a fiber with zero inclination and thus producing significantly more light than a particle inside the lead.

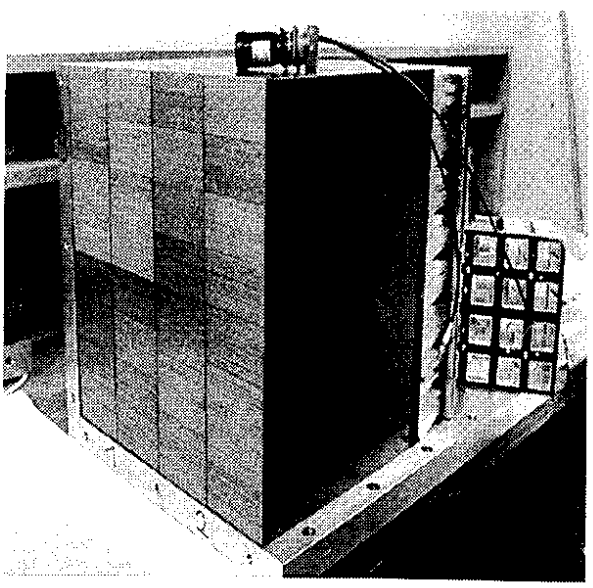

Figure 6. An array of four supermodules.

While this case is not relevant for the H1 Spacal which is an end cap detector, channeling may also occur at angles larger than 0°. This is illustrated in Figure 7.

The particle represented by the arrow on the left side corresponds to the energy spectrum shown in the left histogram. Due to its incidence angle this particle traverses a reasonable mixture of lead and fibers.

In contrast, the particles on the right side, may pass lead only or they may predominantly cross fibers. With a beam of particles entering the calorimeter at this critical angle, the energy spectrum shown in the right histogram is obtained. A double structure is visible, which corresponds to a significantly lower energy resolution.

To reduce any channeling effects in our calorimeter, we vary the submodule orientation depending on their detector position in a way that critical angles are avoided. Thus the supermodules may contain vertically or horizontally stacked submodules or both.

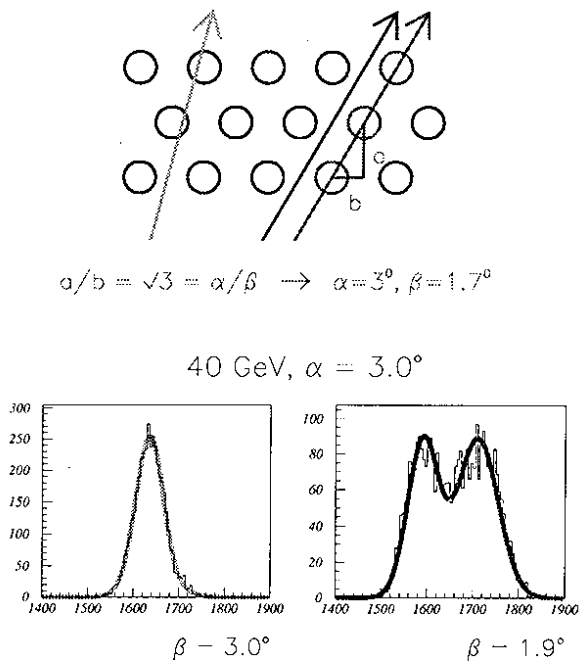

Figure 7. A schematic demonstration of the channeling effect. The angles α and β correspond to the vertical and horizontal inclination of the detector axis with reference to the beam.

3.4. Detector assembly

The r–ϕ view of the Spacal is shown in Figure 8. The circle in the center of the plot represents the beam pipe, which is surrounded by a special module, the insert. The main part of the Spacal is built up of 60 supermodules. At the outer borders a number of special border modules were constructed to minimize the gaps due to the

round shape of the detector. The detector itself is contained in an 8 mm thick aluminium vessel.

To install the Spacal around the beam pipe, the modules above the beam pipe can be removed. These modules are hold by four 2 $\times$25 μm thick steel bands fixed at the top of the detector. Thus these modules will not put any pressure on the insert and consequently the HERA beam pipe.

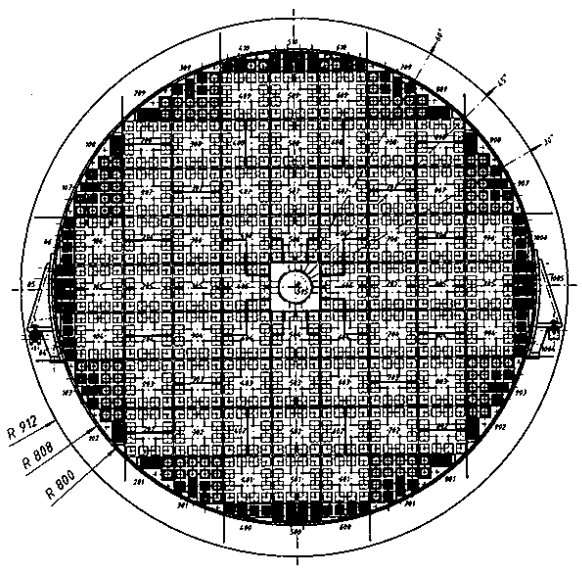

Figure 8. The r–ϕ view of the Spacal.

4. THE HADRONIC SECTION

The hadronic section of the Spacal is built using the same techniques as for the electromagnetic one. Its main purpose is to improve the measurement of hadrons to provide a complementary determination of the kinematic variables y and Q^2 and to suppress photoproduction background events by improving the electron–pion separation. Due to the limited space available for both sections, the hadronic section is only 1.2 interaction lengths deep. The number of interaction length of both calorimeter sections is 2.2 Λ.

For the hadronic section the lead to fiber ratio is 4:1. The same fiber type as for the electromagnetic section was used but with a fiber diameter of 1.0 mm. The hadronic section consists of 120 standard cells with a cross section of 12 $\times$ 12 cm^2.

5. PHOTOMULTIPLIERS AND CALIBRATION SYSTEM

The light readout system of the Spacal has to be operated within a magnetic field of approximately 1.0 T. Thus photomultipiers with a standard dynode structure can not be used. A high gain, a low noise level to be sensitive to minimum ionizing particles and a very precise timing are important design goals of the detector. This excludes the use of photodiodes compared to the current BEMC. Our choice was the fine–mesh–multiplier R5505 from Hamamatsu [7,8]. Within a magnetic field of 1.2 T this multiplier achieves a gain of typically 10^4, approximately a factor 100 less than with no field. The gain dependence on the magnetic field as well as the cathode uniformity with and without field of all multipliers have been investigated in detail. These measurements served as quality control and did determine the final PMT position inside the detector.

The short term stability of the photomultiplier gain is monitored by a light calibration system situated at the back side of the calorimeter. Light from two different LEDs is fed through light guiding fibers into the light mixers. The stability of the LED light ouput itself is measured by additional photodiodes. The system will also provide the initial timing adjustment of all detector channels.

6. HIGH VOLTAGE SUPPLY

The high voltage of the photomultipliers is controlled by 16-channel HV–boards following the design of [13]. Each board is supplied by one global high voltage but the different channels may be regulated individually via an opto–coupler within a range of 360 Volts. Thus by means of a bus system the number of HV cables is reduced to 75.

7. ELECTRONICS

The photomultiplier signal is integrated by an emitter–follower positioned inside the housing tube of the PMT together with the high voltage divider. The detector signal is then distributed into the readout system and the trigger branch. The readout is performed by an analog card with shaping and sample/hold functions followed by the standard H1 calorimeter readout chain [14].

The trigger branch signal enters a Pole–Zero–Compensation circuit followed by a Constant Fraction Discriminater which allows us to compare the time of flight of the calorimeter particles with the nominal collision time of genuine electron–proton events. For 'in–time' events a cluster search is performed by the 'Inclusive Electron Trigger'. The 'Inclusive Electron Trigger' compares the total energy of all possible combinations of four neighbouring cells to different energy thresholds. This provides the trigger for deep inelastic scattering events with an 'in–time' resolution of approximately 1 ns. By discriminating the out–of–time energy, beam gas and beam wall background events can already be rejected at the first trigger level.

8. PERFORMANCE OF THE SPACAL

The performance of final detector modules was tested in various test environments. The light yield of the detector was found to be (2.8 ± 0.3) photoelectrons/ MeV by comparison with a LED. The detector response to minimum ionizing particles is equivalent to 400 MeV. The modules were submitted to beam measurements at the CERN SPS and PS beam lines as well as at DESY. In Figure 9 the energy resolution of one of the first final design modules is shown in dependence of the beam energy. The module was tilted with respect to the beam direction by 3° horizontally and 3° vertically to avoid channeling. We determined the sampling term to be $(7.1 \pm 0.2)\%/\sqrt{E(\mathrm{GeV})}$ and the constant term to be $(0.6 \pm 0.2)\%$ if added in quadrature. Thus at electron energies of 30 GeV the resolution is well below 2% for fixed impact positions.

Horizontal and vertical scans across the module surface have been evaluated with the precise space information of a MWPC as reference. A space resolution of (2.8 ± 0.2) mm/ $\sqrt{E(\mathrm{GeV})} \oplus$ 0.4 mm was determined.

The time resolution was measured at the CERN PS for 4 GeV electrons, interacting pions and minimum ionizing particles. The design time resolution of 1 ns was reached with the final electronics.

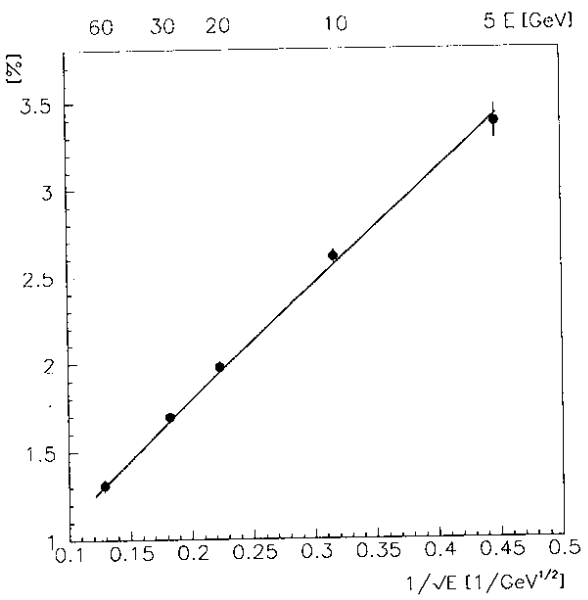

Figure 9. The energy resolution of a final calorimeter module as measured at the SPS at CERN.

During the production the quality of the detector modules was permanently monitored on a computer controlled β–source test bench built by the Institute LPNHE at the University of Paris VI and VII [11]. The collimated β–source is scanning in 1 to 2 mm steps across the front side of the modules moved by a high precision step motor. The resulting photomultiplier current is recorded. A typical example of the uniformity profile of a detector module presented as a lego plot is shown

in the upper part of Figure 10.

The vertical coordinate corresponds to the normalized photomultiplier current, summed over all channels, the other axes indicate the β-source position. In the lower part of Figure 10 the projection to one of the space coordinates is shown. The border between to adjacent cells is indicated by the vertical line at an x value close to 20 mm. For this cell boundary the uniformity is excellent. Note, that the remaining fluctuations of a few per cent can entirely be explained by the light yield fluctuations of the individual fibers.

All standard supermodules and examples of all types of special modules were scanned with the test bench. The scan data should enable us to correct the local inhomogeneities observed at the boundary between some submodules. Inhomogeneities between the border of adjacent cells within a submodule are much less frequent and generally small.

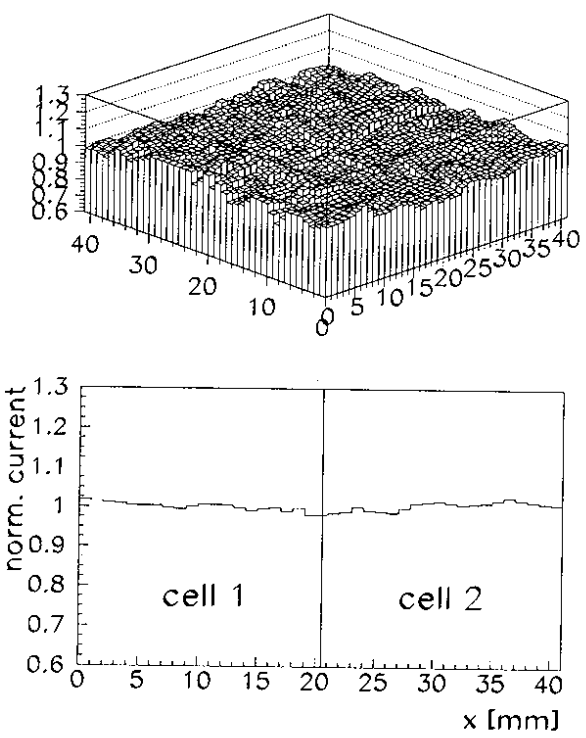

Figure 10. Uniformity profiles obtained with the β-source test bench. The current axis is strongly zero-suppressed

9. SUMMARY

The new spaghetti calorimeter of the H1 collaboration will be installed winter-shutdown 94/95 in the H1 detector. The detector combines compactness and good energy resolution. The lead to fiber ratio of 2:1 together with a fiber diameter of 0.5 mm is at the limit of what is technically possible. The H1 spaghetti calorimeter was designed and constructed within less than two years after its official proposal. The main design goals have, however, successfully been confirmed in both test beam and β-source measurements of final modules. We are looking forward to the first experience of operating the detector in genuine electron-proton collisions.

10. ACKNOWLEGDEMENTS

It is a pleasure to thank my colleagues and the many engineers and technicians from the participating institutes outside DESY for their outstanding commitment and their good team spirit. Their excellent work made the successful realization of the ambitious Spacal project possible. Many thanks to the organizers of the '94 Beijing Calorimetry Symposium' for the pleasant stay in China and the participation in their very interesting conference.

REFERENCES

1. J. Bartels and J. Feltesse, QCD at low x, Proceedings of the Workshop: Physics at HERA, DESY, Hamburg, Germany (1991).
2. H1 Collaboration, Technical Proposal to Upgrade the Backward Scattering Region of the H1 Detector, DESY PRC 93/02.
3. H1 Collaboration, Measurement of the Proton Structure Function $F_2(x, Q^2)$ in the Low x Region at HERA, Nucl. Phys. B407 (1993) 515.
4. R. D. Appuhn *et al.*, Electromagnetic Calorimetry with Lead Fluoride Crystals, Nucl. Instr. Meth. A 350 (1994) 208.

5. S. Dagoret *et al.*, Nucl. Instr. Meth. A 346 (1994) 137.
6. The KLOE collaboration, A general Purpose Detector for DAΦNE, LNF-92/-019 (1992).
7. J. Janoth *et al.*, Response of Mesh-Type Photomultiplier Tubes in Strong Magnetic Fields, Nucl. Instr. Meth. A 350 (1994) 221.
8. R. D. Appuhn *et al.*, Performance Tests with a Large Sample of fine Mesh Photomultipliers for Use at 1.2 Tesla, Proceedings of the IV International Conference on Calorimetry in High Energy Physics, La Biodola, Elba, Italy (1993).
9. A. Walther and R. Barschke, Studies of Scintillating Fibres for a Spaghetti Calorimeter to be used for the H1 Backward Upgrade Project, Proceedings of the Workshop on Scintillating Fiber Detectors, Notre Dame University, Indiana (1993).
10. R. Barschke, Diploma Thesis, University of Hamburg, Germany, unpublished (1994).
11. D. Lacour, Rapport de Stage DEA, LPNHE, Universites Paris VI et VII, September 1992.
12. F. Lehner, Diploma Thesis, University of Hamburg, Germany, unpublished (1994).
13. W. Stamm *et al.*, A low cost HV controller for PMTs, Nucl. Instr. Meth. A 328 (1993) 601.
14. B. Andrieu *et al.*, Nucl. Instr. Meth. A 336 (1993) 460.